

The in-orbit wavelength calibration of the HRC G800L grism

A. Pasquali, N. Pirzkal, J.R. Walsh
July 8, 2003

ABSTRACT

G800L grism spectra of the Wolf-Rayet star WR45, obtained with the High Resolution Channel (HRC) during the Servicing Mission Orbital Verification (SMOV) tests, are presented. The target has been observed in five different positions across the HRC field of view in order to quantify the field dependence of the grism physical properties and wavelength solution. By applying the calibration procedure already used for the grism coupled with the WFC (cf. Pasquali et al. 2003) for non-drizzled spectra, an average dispersion of 24.0 Å/pix in the 1st order, 12.1 Å/pix in the 2nd order, 8.0 Å/pix in the 3rd order, -26.6 Å/pix in the -1st order and -13.4 Å/pix in the -2nd order are obtained. The -3rd order extends only up to ~6500 Å where only one emission line is detected and therefore no wavelength solution can be derived. The amplitude of the dispersion field dependence is about 2% from the centre to the edges of the field of view; the major direction of the dispersion variation is the diagonal from the image bottom right corner to the left top corner. The same trend is observed for all grism orders. We describe the calibration files derived from these SMOV data which are used by the ST-ECF extraction package aXe.

Introduction

The ACS grism available with the Wide Field (WFC) and the High Resolution (HRC) Channels was first calibrated in wavelength during ground tests which made use of a Hg+Ar arc lamp. In the specific case of the HRC, arc spectra were acquired in five positions across the field of view (f.o.v) to check for the field dependence of the spectral dispersion and wavelength zero point. The data analysis showed that the grism

dispersion is indeed a function of position across the HRC field of view, but the amplitude of its field dependence turned out to be only $\sim 2\%$ from the centre to the edges of the chip compared to the 11% measured for the WFC (cf. Pasquali et al. 2003). Consequently, the in-orbit calibrations of the HRC/grism configuration were planned to cover these five “ground” positions with no additional pointing, in order to check the instrument stability and the in-orbit wavelength solution of the HRC/grism configuration.

The wavelength calibration of the HRC/grism was performed during the Servicing Mission Orbital Verification tests by observing the Wolf-Rayet star WR45 (cf. Pasquali et al. 2001). Spectra of the HST standard star GD153 were taken at the same time for flux calibration purposes.

Hereafter, we will discuss the wavelength calibration of the HRC/grism configuration as determined from non-drizzled spectra which have not been corrected for the geometric distortions seen in imaging. The flux calibration for the HRC/grism will be presented in Pirzkal et al. (2003, in preparation).

The Observations

Spectra of WR45 were taken at five different positions across the HRC f.o.v., as illustrated in Figure 1 (Prog. No. 9029, PI Pasquali).

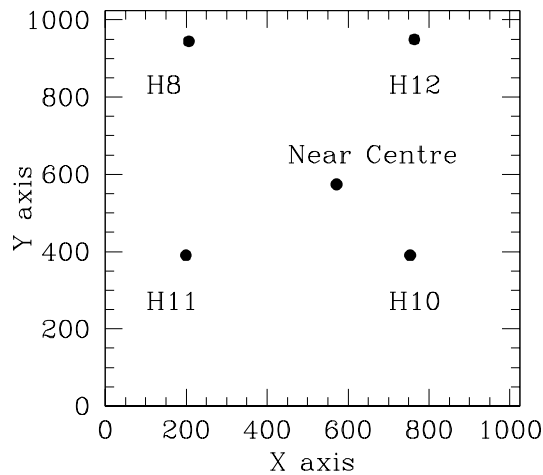


Figure 1: Map of the pointings used for WR45 across the HRC field of view.

Each pointing is described by a pair of image (X,Y) coordinates, and by a pair of POSTARG keywords which give the offsets along the X and Y axes from the centre of the chip (HRC-FIX) in units of arcsecs. The POSTARG values were computed using the equations in Mutchler & Cox (2001). The (X,Y) coordinates of the adopted pointings are listed in Table 1 together with their POSTARG values.

For each position, a pair of direct and grism images was acquired with the direct image taken through the F775W filter. The exposure times are reported in Table 2 for each spectral element, together with the target coordinates.

POINTING	X POSITION (pixels)	Y POSITION (pixels)	POSTARG in X (arcsecs)	POSTARG in Y (arcsecs)
Near-Centre	572	574	+1.61	+1.80
H8	207	944	-8.72	+10.07
H10	754	391	+6.73	-2.26
H11	199	391	-8.94	-3.76
H12	764	949	+7.10	+11.69

Table 1. The (X,Y) coordinates and the POSTARG values of the pointings shown in Figure 1.

Observations were repeated at each position mostly within the same orbit in order to check the repeatability of the filter wheel positioning. This has turned out to be within 2 pixels. A full listing of the HRC direct and grism images is given in Appendix A.

TARGET	RA (J2000)	DEC (J2000)	V mag	F775W	G800L
WR45	11:38:05.2	-62:16:01.0	14.8	3 s	60 s

Table 2. The J2000 coordinates of the SMOV target and the exposure times adopted for each spectral element.

One dimensional spectra were extracted from the grism images with the ST-ECF extraction code aXe (<http://www.stecf.org/software/aXe>). The extraction aperture was set to 2 pixels (consistent with the PSF FWHM in the F775W filter) and the background was measured at a distance of +/- 100 pixels from the spectral trace.

The grism physical properties

A number of parameters are needed in order to locate and trace the spectrum of a source in a grism image: the tilt of the spectra in the grism image, the (X,Y) offsets of the spectral trace from the position of the source in the direct image, the length of the detected grism orders and their separation from the 0th order. These quantities vary across the field of view of the HRC because of the geometric distortions introduced by the inclination of the ACS with respect to the optical axis of HST, and the inclination of the grism itself with respect to the CCD surface. Therefore, the grism physical properties need to be parameterized as a function of position across the HRC f.o.v.

1. The spectral tilt

The slope of the HRC/grism spectra has been measured with respect to the image X axis by fitting the (X,Y) coordinates of the emission peaks (typically 10 positions along the

whole spectral trace) in the observed spectrum of W45 with first order polynomials. The tilts derived from all spectra available at each position have been averaged and the

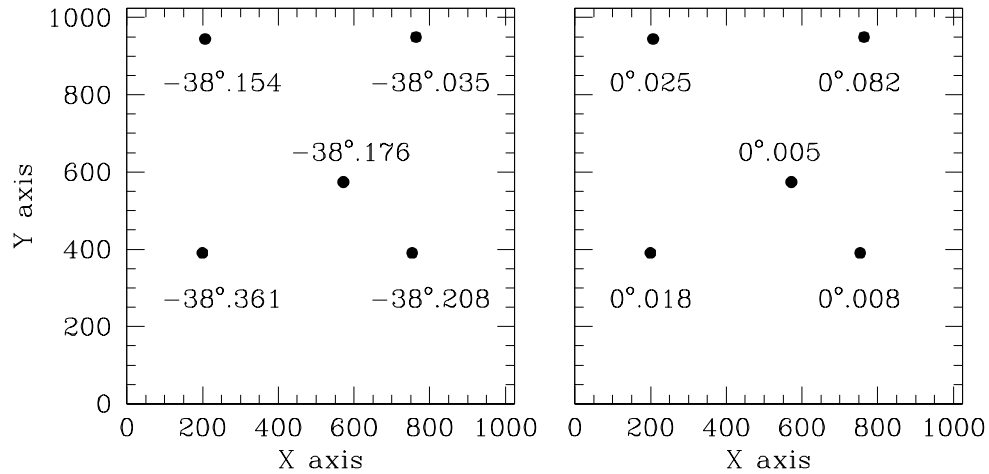


Figure 2: The spectrum tilt (left) and its standard deviation (right) are plotted as a function of position on the HRC chip.

standard deviation of the mean has been computed which takes into account the error of the fits. The RMS of the fits never exceeds 0.3 pixels, which points to highly straight spectral traces when considering an extension of 1020 pixels for the whole grism spectrum in the Near-Centre position. The tilt values are plotted in Figure 2, where the averaged tilts are in the left panel, the corresponding standard deviations in the right one. The spectral tilt decreases from the H8 to the H10 position by $0^{\circ}.05$, and from the H12 to the H11 position by $0^{\circ}.33$, i.e. 1% of the tilt measured in the Near-Centre position. While the variation along the H8 - H10 diagonal is within the error of the fits, the variation in the H12 - H11 direction is significant at 4σ with $\sigma=0.082$ (H12), and is most likely due to the geometric distortions of the HRC. The spectral tilt of the HRC/grism, averaged across the field of view, is $-38^{\circ}.19 \pm 0^{\circ}.12$.

2. The (X,Y) offsets

In addition to the object position in the direct image and the spectra tilt, a third parameter is necessary to locate the spectrum of a given object in the grism image: the offset of the object Y coordinate from the spectral trace. To the X coordinate of the object in the direct image, a Y coordinate (Y_{sp}) is associated along the spectral tilt which is given by the best fit to the spectral tilt. The difference between this Y_{sp} and the object Y coordinate in the direct image is what we call the Y-offset, whose averaged value among the observations available for each pointing is plotted as a function of position across the HRC f.o.v. in Figure 3 in units of pixels, together with its standard deviation. A trend of the Y-offset becoming larger can be seen along the diagonal from the H10 to the H8 positions.

Another pair of coordinate offsets can be also derived, which describe the distance of the grism 0th order in the grism image from the object position (= light centroid) in the direct image along the image X and Y axes. These offsets are listed in Table 3 in units of pixels.

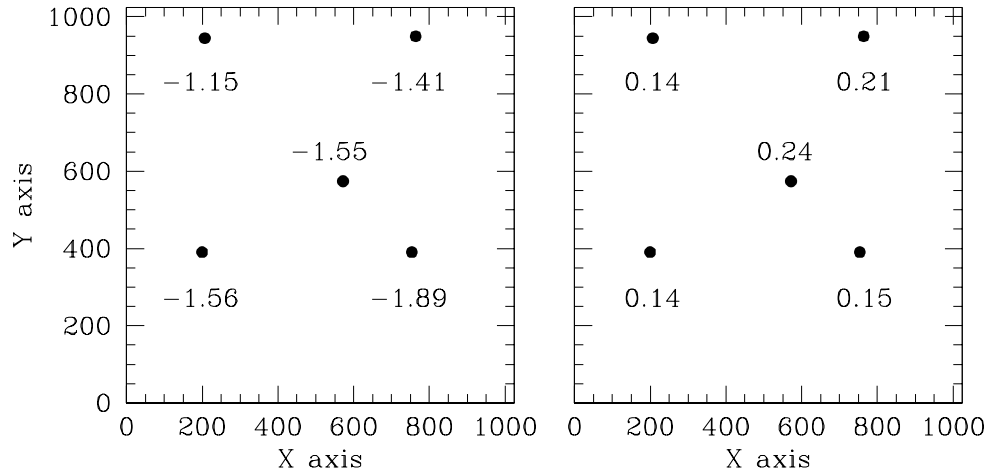


Figure 3: The offsets of the object Y-coordinate (in the direct image) from the spectral trace in the grism image. Units are pixels.

POINTING	ΔX (0 th ord. - Obj)	ΔY (0 th ord. - Obj)
Near Center	-144.98	+112.59
H8	--	--
H10	-146.10	+113.95
H11	-144.90	+112.99
H12	--	--

Table 3. The offsets along the X and Y axes between the grism 0th order and the object position in the direct image. Units are pixels.

3. The length of the grism orders

The extraction of the different orders in a grism spectrum also requires that the length of the grism orders and their separation from the 0th order are known. These quantities are measurable in the grism image directly, once the level of the background has been set. We have fixed the threshold at 3σ level above the background, so that pixels with higher fluxes are flagged as belonging to the object spectrum. No field dependence can be seen in the length of the grism 1st order across the HRC f.o.v. contrary to the higher orders, whose length is truncated as they partially or fully fall outside the physical edges of the image frame. This, of course, depends on the object position in the direct image. The length and

separation of the individual orders from the 0th order along the X and Y axes are reported in Table 4. These values are averaged over the pointings where truncation does not occur.

ORDERS	LENGTH in	LENGTH in	SEPARATION	SEPARATION
	X (pix)	Y (pix)	in X (pix)	in Y (pix)
+1st	153	121	171	-134
+2nd	152	121	341	-269
+3rd	474	374	519	-409
-1st	-143	115	-170	132
-2nd	-136	108	-336	264
-3rd	-70	55	-517	406

Table 4. The mean order length and separation from the 0th order. Typical standard deviations are 3 pixels.

The separation of the individual orders from the 0th order is defined as the distance of the bluest edge of the higher orders from the centroid of the 0th order. The 0th grism order has an averaged length of 6 pixels along both the X and Y axes.

The wavelength calibration: the method

Wavelength solutions based on arc-lamp spectra were already determined during the ground calibrations for the same H8, H10, H11, H12 and Near-Centre positions. They were applied to the extracted spectra of WR45 taken during the SMOV tests, with the purpose to measure the mean FWHM in Å of the WR45 lines. This was in turn used to “degrade” the available high-resolution spectrum of WR45 (cf. Pasquali et al. 2001) to the grism resolution of the HRC, in order to produce a template spectrum at the same resolution of the observations. The line-centroid wavelengths were measured in the “degraded” template spectrum and fitted against the line peaks in pixels (scaled to the X position of WR45 in the direct image) in the extracted spectra.

The fits for the +1st order were performed using a second-order polynomial (with the IRAF routine POLYFIT) since seven lines could be identified. For the higher orders and the negative ones, the fit assumed a first-order polynomial because of the smaller number of lines and the lower S/N ratios.

This procedure was applied to each grism order spectrum obtained at each pointing; dispersion corrections derived for the same grism order and pointing were then averaged. The final results, which are stored in a configuration file for the ST-ECF extraction package aXe (<http://www.stecf.org/software/aXe/index.html>), are presented in the next section.

In the raw, extracted spectra of WR45 the line FWHM is on average 4 pixels for the 1st and -1st orders and 6 pixels for the 2nd order. It turns out to be ~30% larger than the line FWHM measured in the arc lamp spectra acquired during ground calibrations.

The wavelength calibration: the results

The grism 1st order

The grism 1st order spectrum of WR45 obtained at the Near-Centre position is shown in Figure 4, in units of Counts and Angstroms.

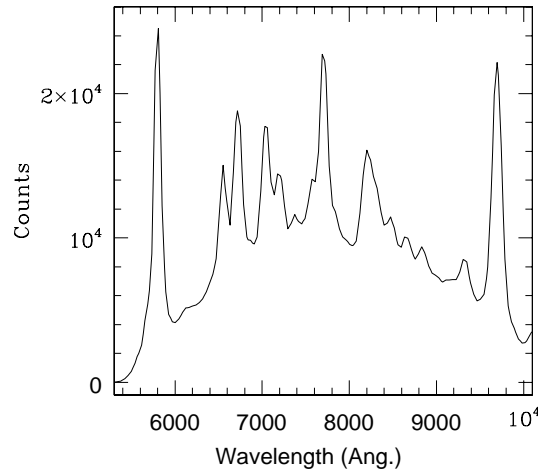


Figure 4: The grism 1st order spectrum of WR45 extracted in the Near-Centre position.

The wavelength solution determined for the grism 1st order is a second order polynomial of the form: $\lambda = \Delta\lambda_0 X' + \Delta\lambda_1 X'^2 + \lambda_0$, where X' is the distance along the spectral trace from the X_0 coordinate of the object in the direct image, i.e. $X' = X/\cos(\text{tilt})$ where X indicates the columns in the grism image (cf. Pirzkal et al. 2003). The dispersion, second term of the dispersion and the zero point are plotted in Figure 5 as a function of position across the HRC f.o.v (left column) together with their uncertainties (right column) which propagate from the errors due to the fitting procedure. A wavelength solution averaged among those in Figure 5 is presented in Table 5 together with the typical RMS of the fitting procedure.

The mean dispersion of the grism 1st order is 24 Å, corresponding to a resolving power R (per resolving element, i.e. 2 pixels) of about 156 at $\lambda = 7500$ Å, a factor of 1.5 higher than the resolving power of the grism 1st order with the Wide Field Channel (cf. Pasquali et al. 2003). Our definition of resolving power requires here a word of caution. Since the FWHM of the lines in the grism spectra are not purely instrumental, but convolved with

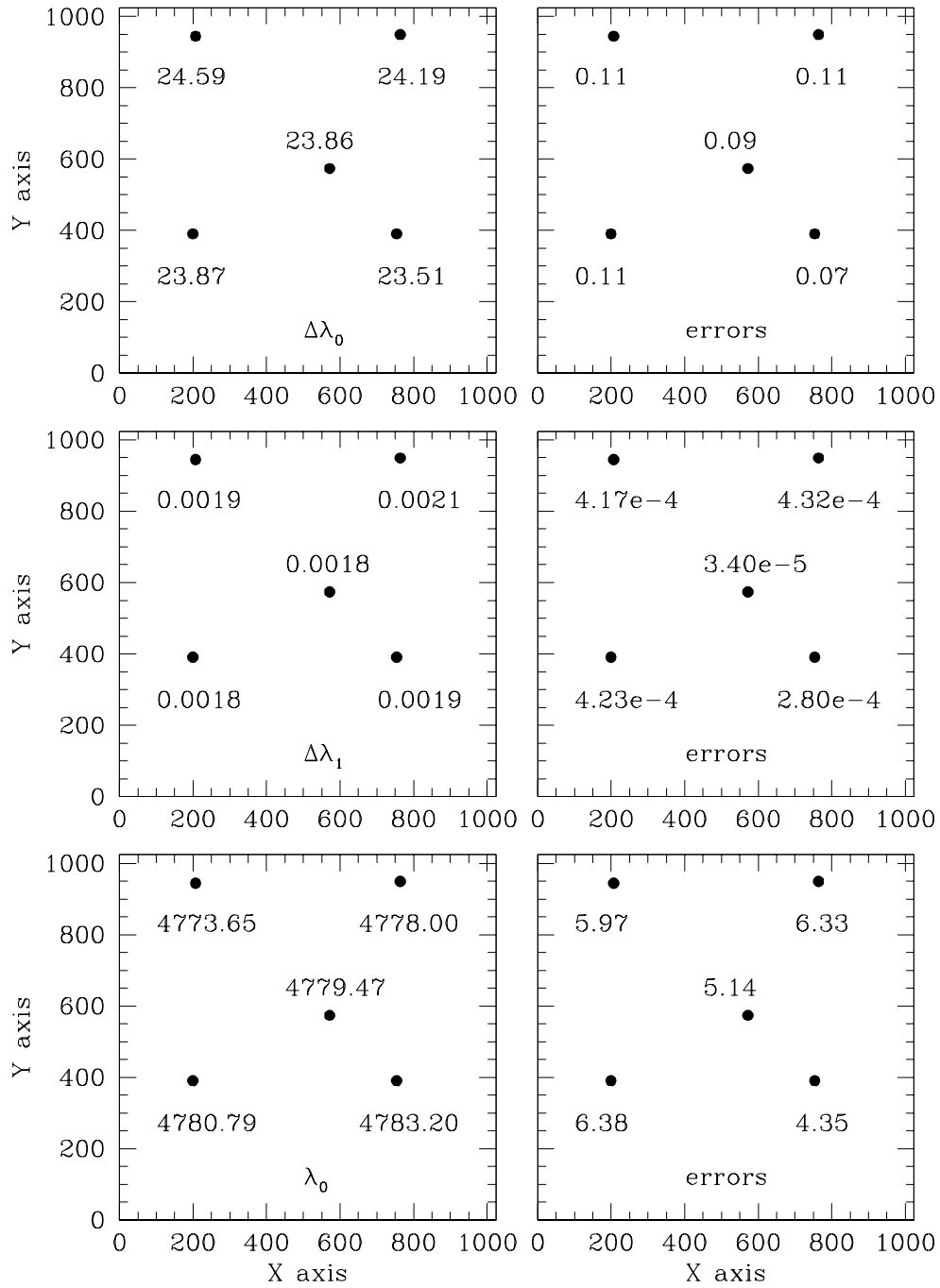


Figure 5: The wavelength solutions computed for the HRC/grism as a function of position across the HRC field of view. All the values are averaged among the several spectra taken for each pointing (left column) and their uncertainties are plotted in the right column.

PARAMETERS	MEAN	ERROR
$\Delta\lambda_0$ (Å/pix)	24.00	0.04
$\Delta\lambda_1$ (Å/pix ²)	0.0019	1.56e-4
λ_0 (Å)	4779.08	2.54
RMS of the fit (Å)	3	

Table 5. The wavelength solution for the grism 1st order averaged across the HRC field of view.

an intrinsic broadening due to high stellar wind velocity, a resolving power $R = \lambda / \text{FWHM}$ could be misleading. Therefore, $R = \lambda / 2\Delta\lambda$ gives an upper limit to the true resolving power of the grism and is also a measure of the grism sampling more than its resolution.

Looking at the upper panels of Figure 5, we notice that the dispersion $\Delta\lambda_0$ varies by ~4% of the value at the centre of the field from the H10 (bottom right corner) to the H8 (top left corner) position. The amplitude of this variation (1.08 Å/pix) is at 10σ level (adopting an uncertainty of 0.11 Å/pix as in the case of the H8 position) and has to be considered real rather than an artifact of the fitting procedure. In other words, a field dependence exists in the dispersion which decreases the grism resolution along the diagonal from the bottom right corner to the top left edge of the HRC field of view. For the sake of comparison, the dispersion field dependence in the HRC has an amplitude a factor of ~5 smaller than in the WFC and the trend is along the same diagonal of the field of view to the WFC but in the opposite direction (cf. Pasquali et al. 2003).

The field variation of the zero point (λ_0) behaves similarly to the dispersion $\Delta\lambda_0$ and the variation (~0.2% of the value in the Near-Centre position) is at 2σ level (assuming $\sigma = 6$ Å from Figure 5 bottom right panel) along the H10-H8 direction.

The grism 2nd order

An example of a 2nd order grism spectrum as obtained for WR45 in the Near-Centre position is plotted in Figure 6.

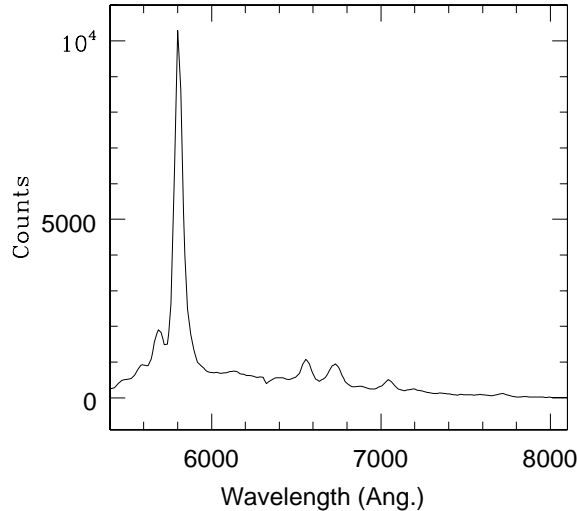


Figure 6: The 2nd order grism spectrum of WR45 obtained in the Near-Centre position. Units are Angstroms and Counts.

The dispersion correction for the grism 2nd order is parametrized with a first order polynomial in the form of: $\lambda = \Delta\lambda_0 X' + \lambda_0$. The wavelength solutions derived for the five adopted pointings are shown in Figure 7.

This order overlaps with the 1st order at about $\lambda = 5400 \text{ \AA}$ and its sensitivity response becomes very low redward of 8000 \AA . The dispersion correction of the 2nd order averaged across the field of view is summarized in Table 6, where the listed errors on the mean parameters take into account the fit uncertainties. The mean dispersion of the grism 2nd order is 12.07 \AA/pix , corresponding to a resolving power R of about 269 at $\lambda = 6500 \text{ \AA}$, a factor of 1.5 higher than the WFC 2nd order (cf. Pasquali et al. 2003).

The dispersion $\Delta\lambda_0$ varies by $\sim 4\%$ of the value in the Near-Centre position from the H10 to the H8 position. The amplitude and direction of this field dependence are the same as derived for the grism 1st order. The zero point λ_0 decreases from the H10 to the H8 position by $\sim 0.3\%$ of the value in the Near-Centre position.

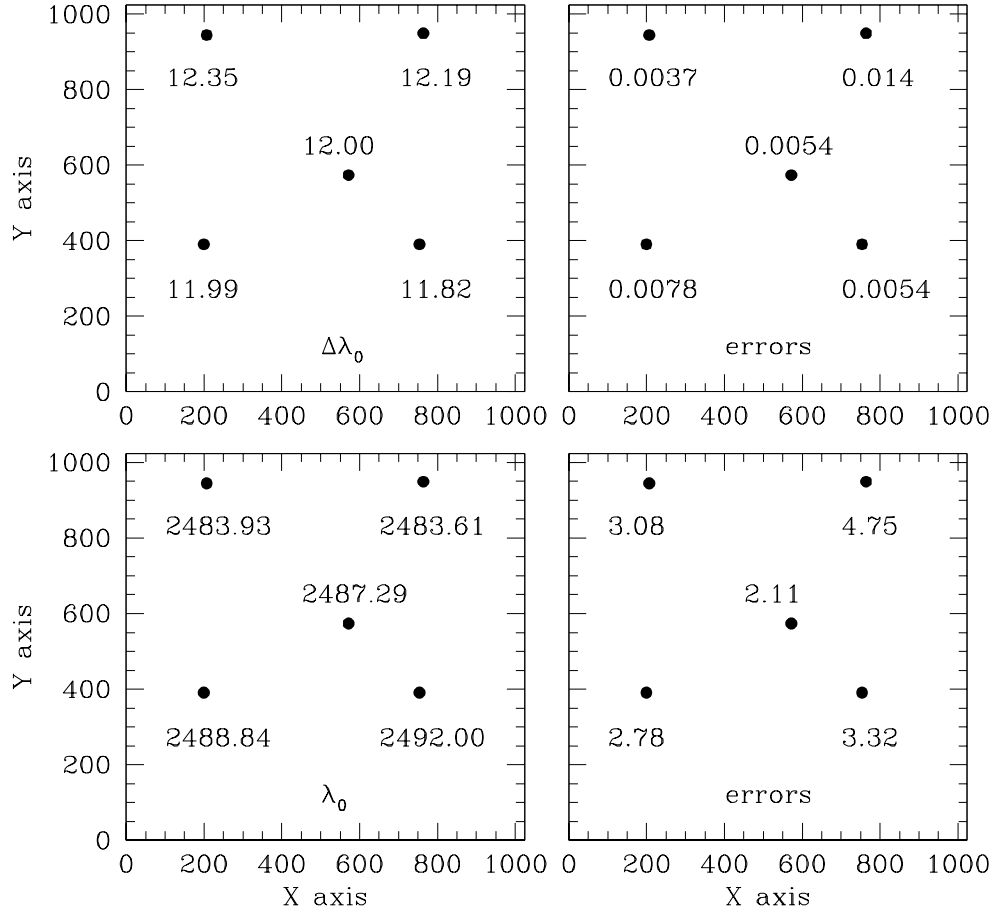


Figure 7: The wavelength solution of the grism 2nd order as a function of position across the field of view. The uncertainties on $\Delta\lambda_0$ and λ_0 due to the fitting procedure are plotted in the right column.

PARAMETERS	MEAN	ERROR
$\Delta\lambda_0$ (Å/pix)	12.07	0.0036
λ_0 (Å)	2487.13	1.48
RMS of the fit (Å)	0.81	

Table 6. The wavelength solution of the grism 2nd order averaged across the field of view of the HRC. The errors, propagated from the fit uncertainties, are shown together with the typical RMS value of the fits.

The grism 3rd order

The grism 3rd order spectra are available only for the Near-Centre, H8 and H11 positions where it appears significantly truncated. Indeed, only two lines are available for the wave-

length calibration, and hence the dispersion correction of the grism 3rd order is a simple first order polynomial: $\lambda = \Delta\lambda_0 X' + \lambda_0$.

The wavelength solutions obtained for the above pointings are reported in Table 7, together with the uncertainties propagating from the fitting procedure.

POINTING	$\Delta\lambda_0$ (Å/pix)	ERROR (Å/Pix)	λ_0 (Å)	ERROR (Å)
Near-Centre	8.07	0.163	1646.43	-
H8	8.06	0.010	1772.23	7.00
H11	7.91	0.006	1731.08	3.14

Table 7. The wavelength solution of the grism 3rd order determined in only three positions across the HRC field of view.

Because of the very small line sample available for the 3rd order, the solutions in Table 7 are just indicative of the resolving power of the order, i.e. $R \sim 437$ at $\lambda = 7000$ Å.

The grism -1st order

Figure 8 illustrates the grism -1st order spectrum of WR45 acquired in the Near-Centre position. The -1st order was detected only in one other position, H10. Its dispersion correction was obtained by fitting a first order polynomial, in the form of: $\lambda = \Delta\lambda_0 X' + \lambda_0$. The available wavelength solutions are reported in Table 8 together with their uncertainties. The mean dispersion is ~ -26.6 Å/pix, which corresponds to a resolving power R of about 140 at $\lambda = 7500$ Å, a factor of 1.5 higher than the WFC.

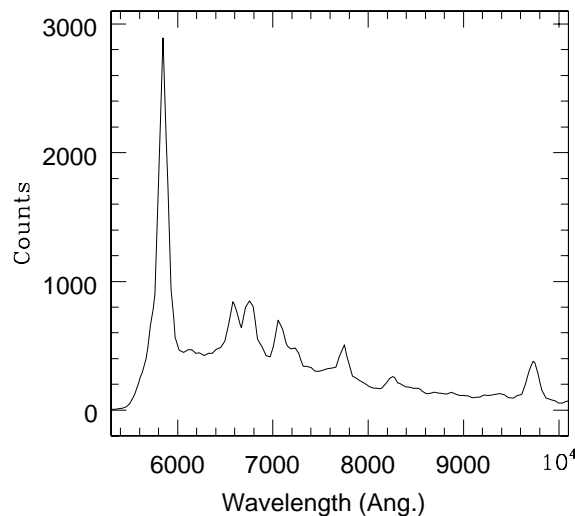


Figure 8: The grism -1st order spectrum of WR45, obtained in the Near-Centre position. Units are Angstroms and Counts.

POINTING	$\Delta\lambda_0$ (Å/pix)	ERROR (Å/pix)	λ_0 (Å)	ERROR (Å)	RMS (Å)
Near-Centre	-26.75	0.03	-5208.84	15.17	5
H10	-26.40	0.01	-5217.70	10.26	3

Table 8. The wavelength solutions of the grism -1st order in the Near-Centre and H10 positions. The errors are related to the uncertainties propagating from the fitting procedure.

The grism -2nd order

The grism -2nd order spectrum is detected in only two positions, the Near-Centre and H10. As in the case of the 3rd order, the -2nd order spectrum is significantly truncated and only two lines can be used for its wavelength calibration. The wavelength solutions derived for these two pointings are listed in Table 9, together with the errors due to the fitting method.

POINTING	$\Delta\lambda_0$ (Å/pix)	ERROR (Å/pix)	λ_0 (Å)	ERROR (Å)
Near-Centre	-13.54	0.02	-2776.34	12.03
H10	-13.31	0.01	-2745.81	7.84

Table 9. The wavelength solution of the grism -2nd order computed for the Near-Centre and H10 positions.

Because of the small line sample available for the grism -2nd order, the dispersion corrections in Table 9 are just indicative of the resolving power, i.e. $R \sim 240$.

The calibration files for aXe

The measurements described in the previous sections have been used to create configuration files for the ST-ECF slitless spectra extraction package aXe (Pirzkal et al. 2001). Since aXe is able to handle the field dependence of the extraction parameters, we have modeled it using first order 2D polynomials. The choice of first order polynomials is dictated by the HRC small field of view and by the small number of available pointings across the field of view.

We have separately fitted the tilt, (X,Y) offsets, wavelength zero points and first and second order dispersion coefficients as a function of the (X,Y) position of the target in the direct image. The residuals to the fit are reported in Table 10 for the grism 1st order.

PARAMETER	FIT ERROR
ΔX	0.58 pix
ΔY	0.39 pix
TILT	$0^{\circ}.0005$
$\Delta\lambda_0$	0.046 Å/pix
$\Delta\lambda_1$	0.0002 Å/pix ²
λ_0	4.77 Å

Table 10. The residuals on the fit for the field dependence of the grism 1st order.

A configuration file containing the description of the field dependence of the positive and negative orders of the HRC grism has been written and can be found at <http://www.stecf.org/software/aXe>.

In order to verify the consistency of the procedure to derive the grism wavelength calibration and its field dependence, we have run aXe with the HRC configuration file and re-extracted the spectrum of WR45 acquired at each pointing. The 1st order spectra are plotted in Figure 9, scaled to the same continuum level. The overlap of these spectra occurs in less than 0.2 pixels (i.e. +/- 5 Å from the line centroid).

Conclusions

During the SMOV tests, we observed the Galactic Wolf-Rayet star WR45 with the HRC and obtained pairs of direct and grism images in five positions across the HRC field of view. The aim of these observations was to derive the in-orbit wavelength calibration of the HRC/G800L grism and its field dependence.

The results obtained for un-drizzled grism images can be summarized as follow:

- The grism 0th order is displaced from the target position in the direct image by -145 pixels in X and +113 pixels in Y on average.
- The grism 0th order is on average 6 pixels in extent for both the X and Y axes in the direct image, and has a FWHM of about 6 pixels in the extracted spectra of WR45.
- The spectrum tilt is on average $-38^{\circ}.19 \pm 0^{\circ}.12$ and is field-dependent. It varies by $0^{\circ}.05$ from the H10 to the H8 position, and by $0^{\circ}.33$ from the H11 to the H12 position.
- The line FWHM in the WR45 spectrum is on average 4 pixels in the grism 1st and -1st orders and 6 pixels in the 2nd order.
- The wavelength solution of the grism 1st order is fitted by a second order polynomial with a RMS of about 3 Å. The higher positive and negative orders are instead fitted with

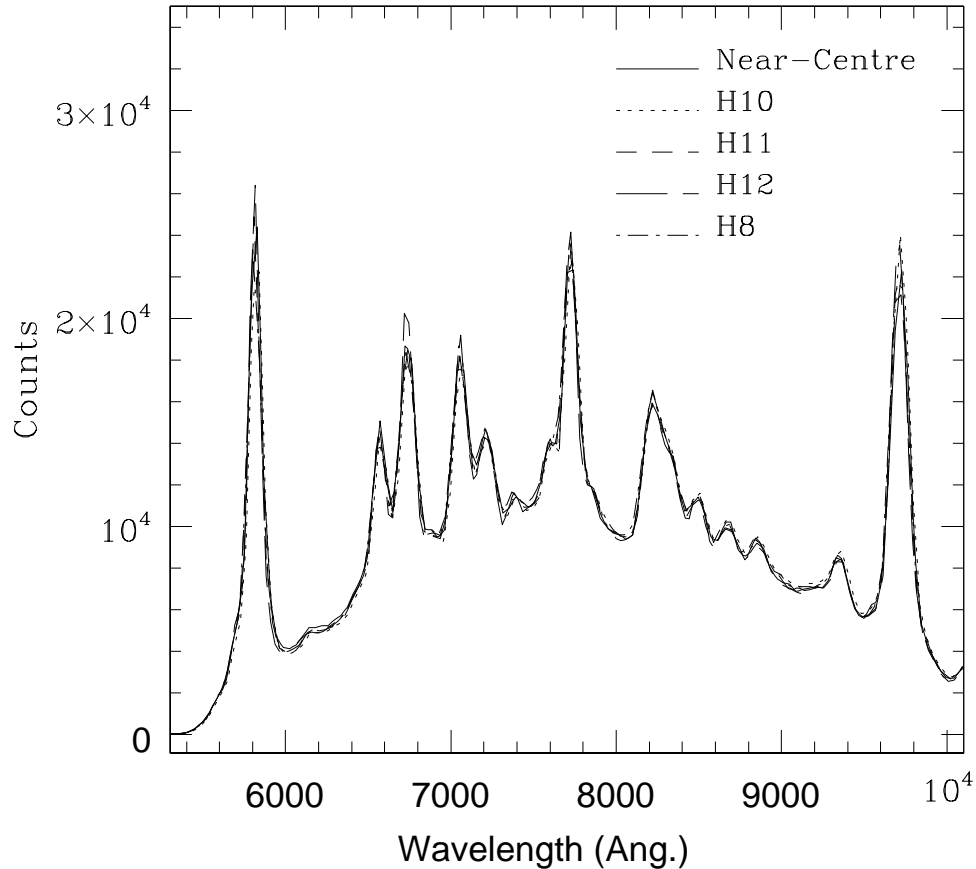


Figure 9: the 1st order spectra of WR45 extracted with aXe and the HRC configuration file.

a first order polynomial with a RMS as high as 3 Å. The wavelength solutions obtained in the Near-Centre position are listed in Table 11.

- The field dependence of the HRC grism properties and the wavelength solution obtained for the various grism orders has been parametrized with a first order 2D polynomial as a function of the target position in the direct image. These 2D polynomials are stored in a HRC configuration file to be used by the ST-ECF spectra extraction package aXe.

References

- Cox, C., Lindler, D., 2002, ISR ACS 2002-02 “ACS Distortion derived from RAS-HOM Measurements”
- Mutchler, M., Cox, C., 2001, STScI ISR ACS 2001-07 “ACS dither and mosaic pointing patterns”
- Pasquali, A., Pirzkal, N., Walsh, J.R., 2001, ST-ECF ISR ACS 2001-04 “Selection of Wavelength Calibration Targets for the ACS Grism”

GRISM ORDER	FIRST TERM DISPERSION ($\text{\AA}/\text{pix}$)	SECOND TERM DISPERSION ($\text{\AA}/\text{pix}^2$)	ZERO POINT (\AA)
First	23.86	0.0018	4779.77
Second	12.00		2487.29
Third	8.07		1646.43
- First	-26.75		-5208.84
- Second	-13.54		-2776.34

Table 11. The wavelength solutions of the grism orders detected in the Near-Centre position.

Pasquali, A., Pirzkal, N., Walsh, J.R., 2003 ST-ECF ISR ACS 2003-01 “The In-Orbit Wavelength Calibration of the WFC G800L Grism”

Pirzkal, N., Pasquali, A., 2001, ST-ECF Newsletter, 28, “SLIM - grism simulator for the ACS”, p. 3

Pirzkal, N., Pasquali, A., Demleitner, M., 2001, ST-ECF Newsletter, 29, “Extracting ACS Slitless Spectra with aXe”, p. 5

Pirzkal, N., Pasquali, A., Walsh, J.R., Hook, R., 2003, aXe User Manual version 1.25 (<http://www.stecf.org/software/aXe/>)

Appendix A

The datasets acquired for the HRC/G800L configuration (Prog. No. 9029, PI Pasquali) are listed in Table 12. The target is WR45.

FITS FILE	ELEMENT	POINTING
j8ca03iiq	F775W	Near-Centre
j8ca03ijq	G800L	Near-Centre
j8ca04acq	F775W	Near-Centre
j8ca04adq	G800L	Near-Centre
j8ca03iaq	F775W	H8
j8ca03ibq	G800L	H8
j8ca03ikq	F775W	H8
j8ca03ilq	G800L	H8
j8ca04aeq	F775W	H8
j8ca04afq	G800L	H8
j8ca03ieq	F775W	H10
j8ca03ifq	G800L	H10
j8ca03ioq	F775W	H10
j8ca03ipq	G800L	H10
j8ca04aiq	F775W	H10
j8ca04ajq	G800L	H10
j8ca03icq	F775W	H11
j8ca03idq	G800L	H11
j8ca04agq	F775W	H11
j8ca04ahq	G800L	H11
j8ca03imq	F775W	H11
j8ca03inq	G800L	H11
j8ca03igq	F775W	H12
j8ca03ihq	G800L	H12
j8ca04aaq	F775W	H12
j8ca04abq	G800L	H12

Table 12. The datasets acquired for the HRC/G800L mode in program no. 9029.